RGNZ/MGPB

Knowledge Driven methods for Cu-Au Porphyry Potential Modelling; a case study of the Mokhtaran area, Eastern Iran

Rudarsko-geološko-naftni zbornik
(The Mining-Geology-Petroleum Engineering Bulletin)
UDC: 136:06
DOI: 10.17794/rgn.2024.3.10

Original scientific paper

Moslem Jahantigh[1]; Hamidreza Ramazi[1]
[1] *Faculty of Mining engineering, Amirkabir University of Technology, Hafiz Street, Tehran, Iran*
[2] *Faculty of Mining engineering, Amirkabir University of Technology, Hafiz Street, Tehran, Iran*

Abstract
Current research investigates multi-criteria decision methods, consisting of AHP TOPSIS, AHP VIKOR and AHP MOORA, to model porphyry copper potential in the Mokhtaran area in Eastern Iran. Evidential layers in this study include intrusive rocks, volcanic rocks, faults, Geochemical mineralization probability index (GMPI), reduction to the magnetic pole of the total magnetic intensity map, argillic and phyllic alterations. The importance of these evidential layers was calculated using the AHP method. Then, a fuzzy method was applied to the same scale the evidential layers. The threshold values of these layers were discretized with the Fractal method. Then, a weight was assigned to each evidential layer. After weighing all of the evidential layers, different MCDM methods, including AHP TOPSIS, AHP VIKOR, and AHP MOORA, were implemented to combine these layers and outline the Porphyry Copper Prospectivity Models. The predicted models show the same promising areas. The appropriate coincidence can be seen between high potential areas and mine indications. Then the success curve rate was implemented to compare the three predicted models. Based on this method, the AHP TOPSIS has a better performance. Since the success rate curve belongs to AHP TOPSIS, it is placed above the other two methods. Next, AHP VIKOR has a better performance than AHP MOORA. The three MCDM methods produced the same Cu porphyry mineralization areasd along fault zones.

Keywords:
AHP; MOORA; VIKOR, Mokhtaran; Porphyry

1. Introduction

Identifying high-potential areas is an essential part of geoscience research studies and effectively explores and introduces occurrences of economic deposits. Different methods, including geochemistry, geophysics, remote sensing, and geology, are applied to model high potential areas in wide geological environments (**Abedi et al., 2016**). Mineral potential mapping is usually considered a multi-criteria decision-making (MCDM) method because it generates a mineral potential model. These predictive maps are generated using different evidential layers (Abedi et al. 2016). The application of MPM can decrease risk and uncertainty (**Li et al., 2020; Parsa et al., 2016**). **Cargill and Clark (1978)** presented mineral potential modelling for the first time. After introducing the concept of MPM, several studies were conducted to integrate geoscience data. Two methods can be mentioned to integrate geospatial data: (1) Expert-oriented (2) data-oriented. The two methods integrate and assign different geospatial data and introduce high-potential areas for future exploration efforts (**Pan and Harris, 2015**). Expert-orented methods use expert experience and knowledge to determine the numerical significance of different geospatial layers. BWM-MOORA (Riahi et al. 2023), FUCOM-MOORA and FUCOM-MOOSRA **(Feizi et al., 2021)** and fuzzy logic **(Du et al., 2021)** methods have been published for mineral prospectivity using knowledge-driven methods. Several statistical and non-statistical decision-making techniques have been applied in MPM. The multi-criteria decision-making methods have been popular and widely applied in recent geoscience research, especially for mineral potential modelling (**Feizi et al., 2021**).

The Mokhtaran area in Eastern Iran is a good case for knowledge driven prospectivity models. Since the explored mineral occurrences in this area are limited, knowledge data driven methods are not appropriate for generating prospectivity models. However, there are sufficient geospatial data for knowledge prospectivity modelling. The Mokhtaran area has high potential for Cu-Au porphyry mineralization. Therefore, this paper can supply target areas and facilitate future works. In this study knowledge-driven methods including AHP VIKOR, AHP TOPSIS and AHP MOORA were applied for Cu-Au prospectivity modelling in the Mokhtaran study area. Then, the application of all of the models were evaluat-

Corresponding author: Hamidreza Ramazi
e-mail address: ramazi@aut.ac.ir

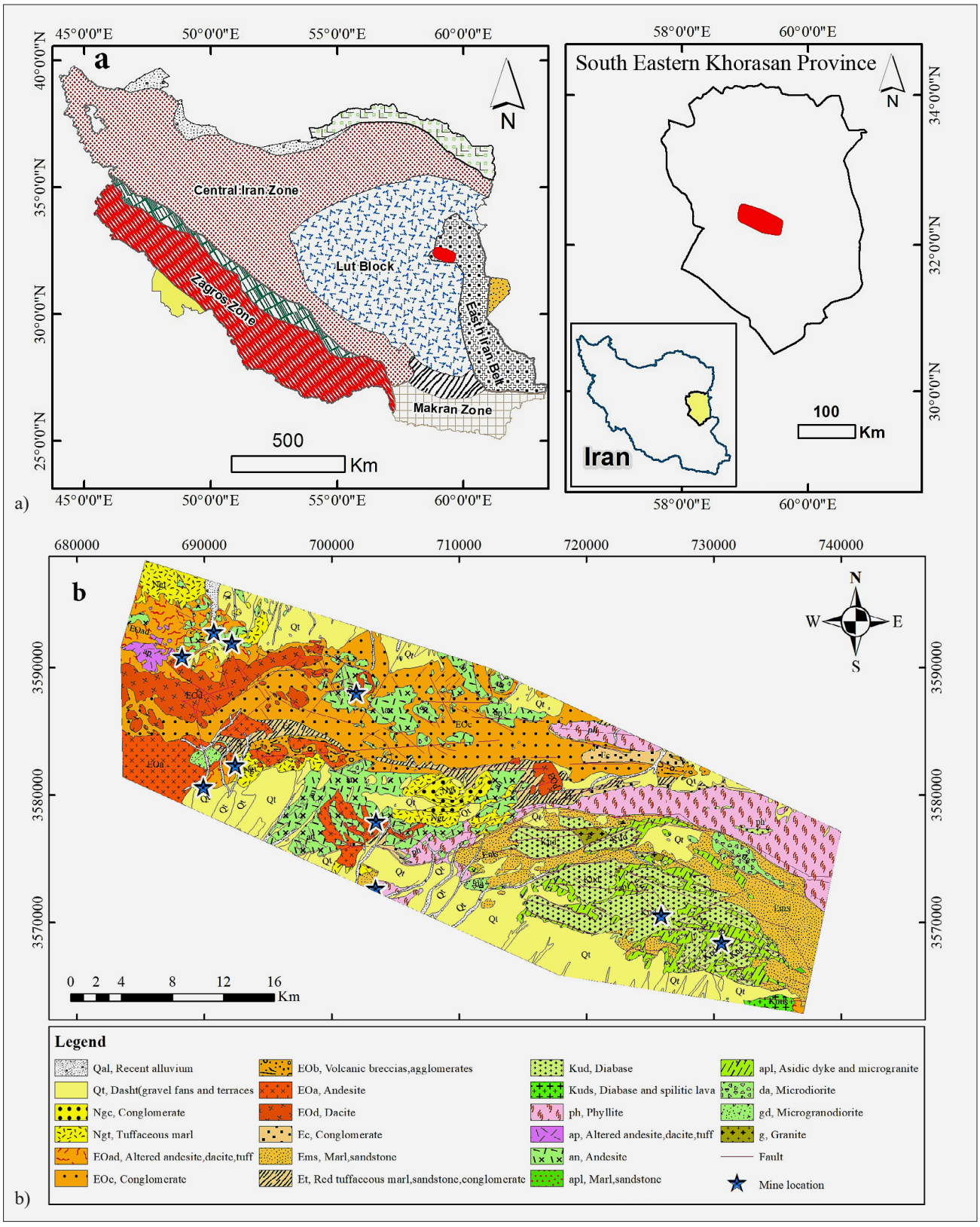

Figure 1: a) Location of the Mokhtaran area in the Lut block, b) geologic map of the study area

ed, and the predictive performance of these models was compared. Several new target areas were revealed in this study, which can facilitate fieldwork for future exploration activities.

2. Geology

Study area is situated in the Lut Block of Eastern Iran **(Figure 1).** The Lut Block is one of several microconti-

nental blocks interpreted to have drifted from the northern margin of Gondwanaland during the Permian opening of the Neo-Tethys, which was subsequently accreted to the Eurasian continent in the Late Triassic during the closure of the Paleo-Tethys (**Shafaroudi et al., 2015**). This region's magmatic and tectonic formation occurred within an extensional process (**Shafaroudi et al., 2015**). The Lut block zone is surrounded by the Nehbandan fault, the Daruneh fault, the Nayband from the east, north and west respectively, and the Urmia-Dokhtar magmatic arc from the south (**Berberian and King, 1981**). There is high potential for different kinds of mineralization in East of Iran; e.g., porphyry, epithermal, and skarn deposits, which is due to the Afghan Cenozoic subduction beneath of the Lut Block. This subduction caused a wide range of magmatic activities during the Eocene and Oligocene and produced different types of igneous rocks with different compositions (**Karimpour et al., 2014**). The Mokhtaran study area is a part of the flysch zone and coloured mélange Belt of East Iran (**Berberian and King, 1981**), exposing varieties of rocks of known or inferred Late Cretaceous age and their tertiary cover. The magmatic intrusions in the area consist of granite, microgranite, microdiorite and felsic dikes. These units belong to the Tertiary period and are intruded in the flysch units. The Paleogene volcanic rocks cover the western part of the area and consist of andesite, dacite, diabase, spilite lavas and tuffs. In the west of this area, the volcanic rocks, especially andesite, are intensively altered. Nortwest-Southeast trending faults have provided appropriate conditions for mineralization in the Mokhtaran area.

3. Conceptual model for Porphyry Cu-Au Deposits

For mineral prospectivity modelling, a dataset should be created that identifies the type of mineralization in any area. To achieve this aim, a conceptual model should be defined based on which the evidential layers are produced. Constructing this model for mineral prospectivity modelling is essential in forecasting mineral resources in regional prospecting. This model is a textual depiction for mineral prospectivity modelling based on various geological exploration theories and data integration to create a model in deposit and regional scales (**Li et al., 2022**). These deposits often occur in magmatic arc settings with calc-alkaline magma series. These magmatic activities belong to the subduction of oceanic crust beneath a continental crust (**Hou et al., 2011**). The metals in porphyry deposits originate from the lower crust and are transferred to shallow surfaces by magmatic stocks and fluids (**Richards, 2011**). These fluids alter the surrounding rocks. Therefore, mineralizing, controlling intrusive bodies, the volcanic rocks that host the mineralization, and producing alterations are key features in porphyry prospectivity modelling. Cu-Au porphyry deposits originate from hypabyssal diorite to quartz diorite and are related to volcanic and subvolcanic rocks such as dacite and andesite (**Sillitoe, 2010**). Some known porphyry mines in the Mokhtaran area, e.g., Maherabad and Khupic, are controlled by granite, microgranite, and monzodiorite (**Almasi et al., 2023**). In the recent study, the proximity maps of intrusive suites and dikes were generated as one of the main factors for Cu-Au porphyry prospectivity modelling.

Volcanic rocks that host porphyry systems were taken from the geology map.to create the proximity map that is used in the modelling process. Porphyry deposits usually are located underneath comagmatic volcanic rocks that are altered by hydrothermal fluids originating from porphyry systems **(Sillitoe, 1973).** Phyllic, argillic, and propylitic alteration assemblages are related to porphyry systems and can be extracted from ASTER data. The most of the reserve is located in the phyllic alteration zone. The mineralization in this zone contains hypogene sulphides, especially bornite and chalcopyrite. Phyllic and potassic zones are the core of a porphyry mineralization, and the argillic zone is formed in the upper central part of the system. Therefore, locating these zones is an essential key in porphyry prospectivity modelling.

Porphyry deposits can be identified through stream sediment geochemical explorations. In several instances, stream sediment geochemistry in areas with known deposits has identified a wide range of deposits **(Coope, 1973).** Therefore, stream sediment geochemistry is an effective tool in regional-scale explorations. Stream sediment samples are analyzed for several elements, which are correlated in mineral systems and can be used as a tool to determine the type of a mineralization. For instance, the appropriate geochemical assemblage of elements related to porphyry deposits is Cu–Au–Mo–Zn–Pb–As–Sb–Ag–Fe–S (**Du et al., 2021**). **Yousefi et al., (2012**) introduced the geochemical mineralization probability index (GMPI) method to discriminate the deposit type. A stepwise factor analysis is implemented to calculate the GMPI. In the first step, the geochemical data is transformed into a normal dataset. Then, the principal component analysis is performed on the normalized data to extract the geochemical factors which contain small areas as high favourability target areas that may overlap with the multi-variate geochemical map. Afterwards, the second factor analysis is carried out to obtain multi-variate geochemical parameters of the porphyry deposits. In each factor resulted from the second factor analysis step, positive element correlation are determined. Therefore, in the third step, a third factor analysis is implemented on the geochemical dataset. So, three sets of factor analyses are calculated. After performing the factor analysis, the weights should be affected on the geochemistry sample to discriminate the type of the deposit. The calculated weight is GMPI.

Besides hydrothermal alterations and magmatic activities, regional tectonic is another effective factor in

MPM. The tectonic setting and structures influence the size and location of the PCDs (**Mirzaie et al., 2015).**

Investigating porphyry copper mineralization from a tectonic point of view indicates that PCDs have occurred within brittle structures. Of course, no unique environment exists to form this kind of mineralization (**Sillitoe, 1997**).

Thus, zones of high lineament density are considered favourable targets for porphyry copper exploration. On the other hand, fault zones are suitable conduits to create of alteration zones and stockwork veinlets. Therefore, faults play an essential role in creating porphyry deposits and hydrothermal alterations. So, the fault density map is considered as an essential key in copper- gold porphyry modelling.

Aeromagnetic surveys can be implemented to outline the location of porphyry Cu–Au porphyry deposits are rich in magnetic minerals, such as magnetite and pyrrhotite (**Sinclair, 2007**). The highly magnetic areas are located in the potassic zone in porphyry deposits. So, this zone produces a high magnetic anomaly in aeromagnetic datasets. These anomalies were included as favourable targets for porphyry copper modelling in this area.

Based on the constructed model, the evidential layer consists of intrusive rocks (granite, microgranite and microdiorite), volcanic rocks, faults, argillic and phyllic alteration zones, multivariate geochemical signatures, and the RTP magnetic map.

4. Methods

4.1. Methods for evidential layer weighting

4.1.1. Fractal

Cheng et al. (1994) presented the fractal method for the first time. Furthermore, this method was widely used in geoscience studies after that; for example, **Cheng et al. (1994); Afzal et al. (2013); Saljoughi et al. (2018); Riahi et al. (2023)**. In a recent study, the fractal method was implemented to calculate the threshold values of evidential layers.

The fractal analysis is written as follows (**Heidari et al., 2013**):

$$S(a\leq\vartheta) \propto \rho^{(-b1)}; S(a\geq v)\propto\rho^{(-b2)} \quad (1)$$

S(ρ) refers to the region where the concentration values exceed the specified value, denoted as a. In this equation, the threshold is denoted as ϑ, and the characteristic exponents are denoted as b1 and b2.

4.1.2. Analytic Hierarchy Process (AHP)

Saaty (1977) first introduced the analytical hierarchy process (AHP), widely recognized as one of the most popular MCDM techniques. **Rosaria and Camanho (2015)** believe that the AHP is a tool to "measurement through pairwise comparisons and relies on the judgments of experts to derive priority scales. The hierarchical decision tree of Mokhtaran is shown in **Figure 2** where tree main creations are considered, including of Geochemistry signature, airborne magnetic anomaly, Geology and remote sensing and eight sub-criteria are considered. These sub-criteria consist of GMPI, RTP, intrusive rocks, volcanic rocks, faults, argillic alteration, phyllic alteration and iron oxide alteration. These criteria and subcriterias were used to make ready evidential layers related to Cu- Au porphyry mineralization.

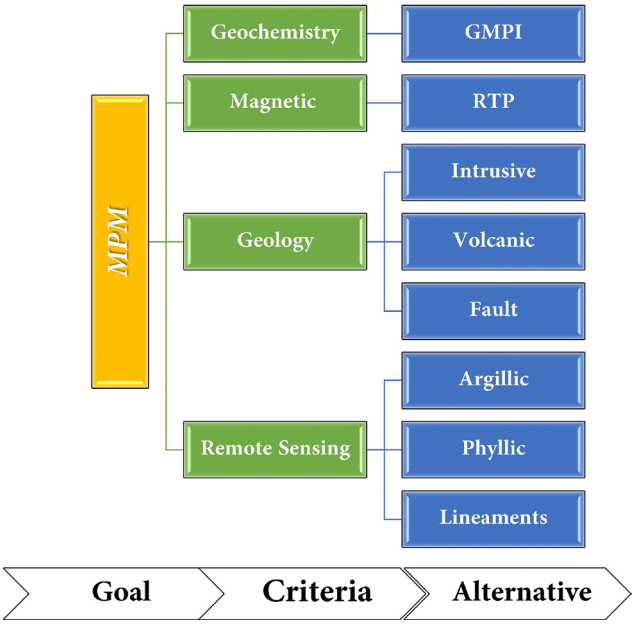

Figure 2: Hierarchy used for prospectivity modeling

4.2. MCDM method for mineral potential modelling

4.2.1. TOPSIS

TOPSIS method was introduced with **Hwang and Yoon (1981)** for the first time. The TOPSIS method is an multi criteria desicin method. The objective of this approach is to select the optimal option with the least proximity to its positive ideal outcome. To determine the TOPSIS value, it is necessary to carry out the subsequent procedures **(Robbi et al., 2018):**

STEP 1: Create decision matrix based on input dataset.

STEP 2: Calculate the normalized decision matrix.

STEP 3: Calculate the weighted normalized decision matrix with AHP method.

STEP 4: Determine the ideal and negative-ideal solution.

STEP 5: Calculate the separation measures, using the n dimensional Euclidean distance.

STEP 6: Calculate the relative closeness to the ideal solution.

STEP 7: Rank the preference order.

4.2.2. VIKOR

VIKOR is an approach to decision-making that is used for addressing problems in discrete spaces **(Siahaan et al., 2018).** The VIKOR method includes of seven steps:

STEP 1: Create a decision matrix based on the input dataset.

STEP 2: Determination of the vector of weights for criteria with AHP method.

STEP 3: Develop a decision matrix that is normalized.

STEP 4: Calculate the best and worst value of each criteria.

STEP 5: Regret and utility values calculation.

STEP 6: VIKOR index (Q) calculation.

The Q value is determined based on the following relation

$S^* = Max(Si)$

$R^* = Max(Ri)$

$$Q_i = v\left[\frac{s_i - s^-}{s^* - s^-}\right] + (1-v)\left[\frac{R_i - R^-}{R^* - R^-}\right] \quad (2)$$

In this equation, $(s_i\text{-}s^-)/(s^*\text{-}s^-)$ indicate the distance rate from the ideal solution, $(R_i\text{-}R^-)/(R^*\text{-}R^-)$ indicate the distance rate from the anti-ideal solution, and the parameter v is selected according to the agreement ratio of the decision maker group. The value of Q is a function of *Si* and *Ri*, which are the distance values from the ideal solution for $P = 1$ and $P = \infty$.

STEP 7: Alternatives sorting due to R, S, Q values

At this point, Q, S, and R are organized into groups of options, beginning with the smallest and progressing to the largest. Ultimately, the choice is made for the superior option, which will be acknowledged as superior in all three groups.

4.2.3. MOORA

The MOORA method is widely regarded as valuable for improving the best alternatives and determining the most viable substitute among a set of options in multi-criteria decision making. To achieve this objective, the subsequent measures need to be implemented:

STEP 1: The process includes developing and producing a decision matrix.

STEP 2: The process includes normalizing the decision matrix.

STEP 3: Determination of the vector of weights for criteria with AHP method.

STEP 4: The process involves enhancing various qualities by incorporating standardized achievement when maximizing (positive qualities) and subtracting when minimizing (negative qualities).

STEP 5: In order to predict a specific event accurately, it is important to consider that certain attributes hold more significance.

5. Dataset

In this study, the spatial dataset consists of

- ✓ Intrusive rocks
- ✓ Volcanic rocks
- ✓ Faults density
- ✓ Stream sediment samples
- ✓ Phyllic alteration
- ✓ Argillic alteration
- ✓ Reduction to pole of aeromagnetic data.

These data were gathered based on the conceptual model. **Table 1** summarizes the spatial dataset used in this paper.

The geological dataset was selected based on intrusive **(Figure 3a)** and volcanic rocks **(Figure 3b).** The intrusive rocks include granite, microgranitic dikes, and microdiorite stocks. These intrusive units have a high potential for Cu-Au porphyry mineralization, as these rocks units have been formed in western parts of the Mokhtaran area. In the east of of the Mokhtaran area, granitic and microdioritic units have intruded into the sedimentary rocks. These intrusive and volcanic units were obtained from the 1:100K geology map of Mokhtaran published by the Geological Survey of Iran (GSI).

Faults and fault zones play a very effective role in porphyry copper mineralization and their hydrothermal alterations. Mineralized indications are located on moderate - to high-density fault zones. The existing faults were also extracted from the Mokhtaran geology map to map their density **(Figure 3).**

In this paper, the data from 44 elements in a stream sediment data set surveyed by the GSI were utilized. The SFA method was then applied three times to enhance the intensity of geochemical signatures in and around min-

Table 1: Overview of spatial data sets utilized in the analysis of mineral predictions

Original information	Source	Process	Evidential layers
Aster Data	USGS	Band ratio 5/7	Argillic alteration
Aster Data	USGS	Band ratio (5+7)/6	Phyllic alteration
Mokhtaran Geology map	GSI	Euclidean distance to intrusive rocks	Proximity to Host rocks
Mokhtaran Geology map	GSI	Euclidean distance to volcanic rocks	Proximity to Host rocks
Mokhtaran Geology map	GSI	Fault Density	High fault density
Geochemistry data	GSI	GMPI	High Geochemistry anomalies
Total magnetic intensity	AEOI	Reduction to pole	High magnetic anomalies

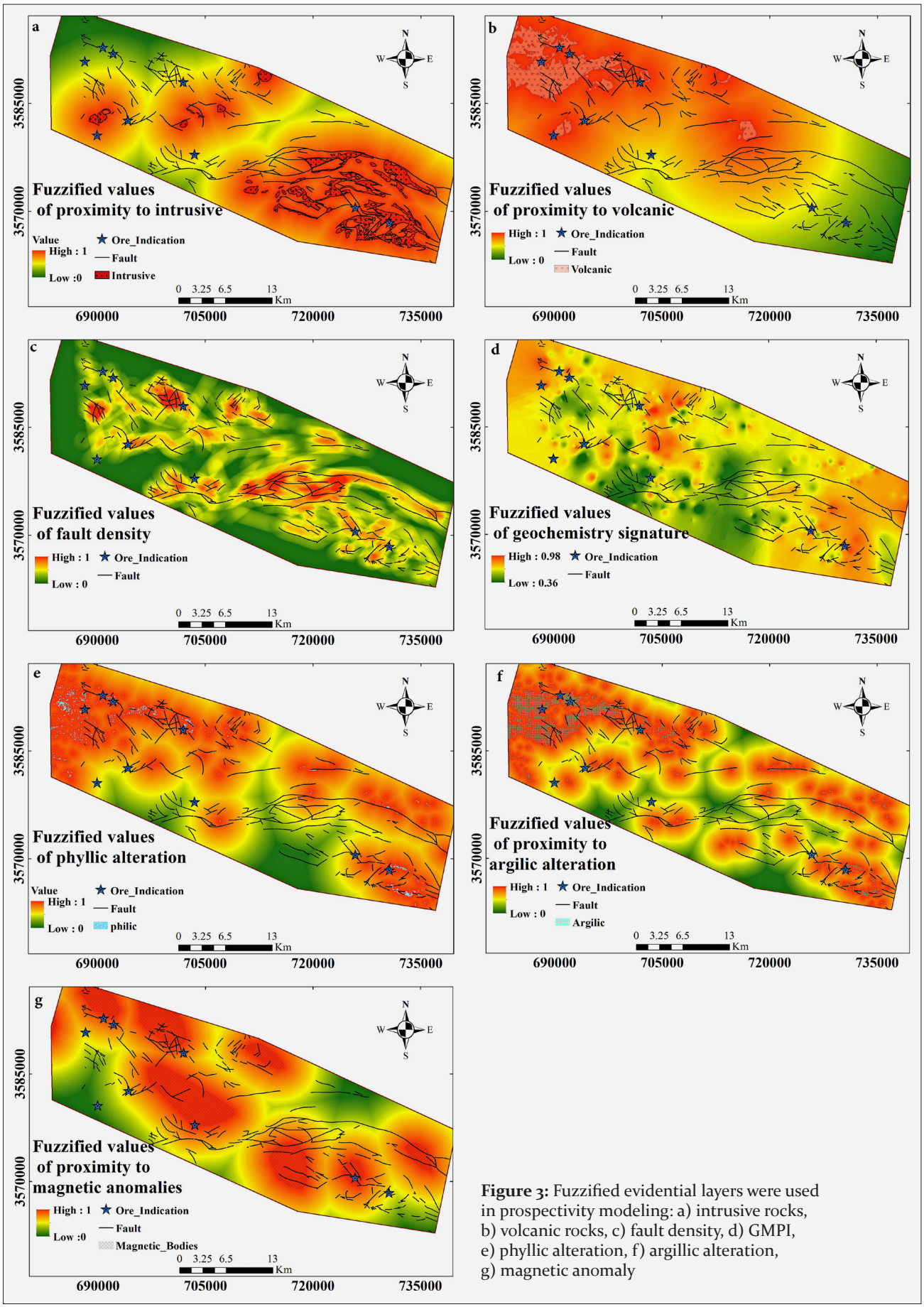

Figure 3: Fuzzified evidential layers were used in prospectivity modeling: a) intrusive rocks, b) volcanic rocks, c) fault density, d) GMPI, e) phyllic alteration, f) argillic alteration, g) magnetic anomaly

eralized zones. It is important to note that this method effectively eliminates the signatures of elements that are not related to porphyry systems. Subsequently, the predicted porphyry-related areas were further intensified. To achieve this objective, a logistic transformation was performed on the resulting SFA map. This involved subtracting the minimum value of the data from the SFA data and dividing the resulting integer by the difference between the maximum and minimum values of the data. Following this, the GMPI method was employed on the transformed data to generate the GMPI map. **Figure 3** displays the GMPI map of the Mokhtaran region, where all mineralized indices are situated in areas with high geochemical signatures.

The alteration zones of the Mokhtaran area were mapped by processing ASTER images. The radiometric and geometric preprocessing corrections were carried out on the data. The argillic and phyllic alteration zones were obtained from Aster data using the band ratio method. The argillic and phyllic alterations were obtained using the ratios of 5/7 and (5+7)/6. The highly altered zones coincide with lineaments and structures and encompass all mineral indications. The proximity maps of argillic and phyllic alterations were drawn based on these results.

The aeromagnetic datasets used in this study have been taken from the Atomic Energy Organization. The line spacing of aeromagnetic data is 500 m, and The height of the harvest was 120 meters. The reduction to pole transformation of total magnetic intensity was used as an evidential layer **(Figure 3).** The reduction to pole map was used to dicrete high magnetic anomalies. Seven high magnetic zones were extracted from aeromagnetic maps, of which five zones coincide with copper mineralization occurrences.

6. Continuous Evidential layer and fuzzification

To create continuous geospatial data, the fuzzified map was produced using the available spatial dataset consisting of (1) multi- variate geochemistry analysis (GMPI), (2) aeromagnetic anomalies, (3) argillic alteration zones, (4) phyllic alteration zones, (5) volcanic rocks, and (6) intrusive rocks. The evidential layers have different scales and should be transformed into the same scale. The linear fuzzified function is used for this purpose. The potential form of the linear membership function is shown in **Figure 4.**

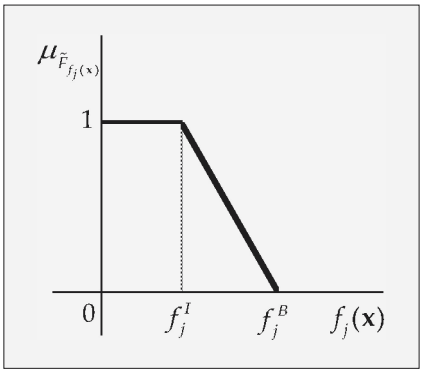

Figure 4: The graph of the linear fuzzy membership function

7. Discrimination of spatial evidential layers through fractal analysis

Cheng et al. (1994) introduced the fractal method. In this paper, the threshold values of fuzzified evidential layers were discrete with the concentration-area fractal method. The concnentration-area log-log of fuzzified evidential layers of argillic alteration, phyllic alteration, subvolcanic rocks, volcanic rocks, RTP magnetic anomalies and fault density were presented in **Figure 5a-d**. Also, C-A log- log of logistic transformed of GMPI was presented in **Figure 4e**. Discriminated maps of evidential layers were produced using the C-A fractal those are shown in **Figure 6.** All evidential layers were discretized in six classes with the fractal method and the log-log curve of every evidential layer.

8. Mineral prospectivity modelling

To combine the eight geospatial datasets originate from airborne geophysics, geology, satellite images and stream sediment datasets, a 105829×7 decision matrix was made from the spatial evidential layers. Every member of this decision matrix belongs to a pixel of the raster file constructed from evidential layers. The csv file of the matrix can be imported to MATLAB software **(Ghezelbash and Maghsoudi, 2018).**

Weighting geospatial data in mineral prospectivity modelling is a matter to consider **(Najafi et al., 2014).** The process of assessing the significance of different evidential layers is called map layer weighting. The AHP method was used to weigh the evidential layer maps. This method is based on the experience and judgment of experts. Achieving proper weights is done by the trial-and-error process. For calculating the weight of evidential layers, first, a decision problem was depicted using intricate hierarchical arrangement (in this study, exploration of porphyry copper deposits) **(Figure 7).** A hierarchy comprises of at least three levels: the initial level represents the objective, the intermediate level encompasses various criteria that determine other options, and the ultimate level contains the decision **alternatives (Albayrak and Erensal, 2004).** Geospatial dataset, along with their discretized values and the values associated with each pixel, were utilized as the criteria, sub-criteria, and alternatives **(Ghezelbash and Maghsoudi, 2018).**

The weights resulting from the AHP method are presented in **Table 2**. All weights are lower than 0.27. The largest weights are proximity to the argillic alteration

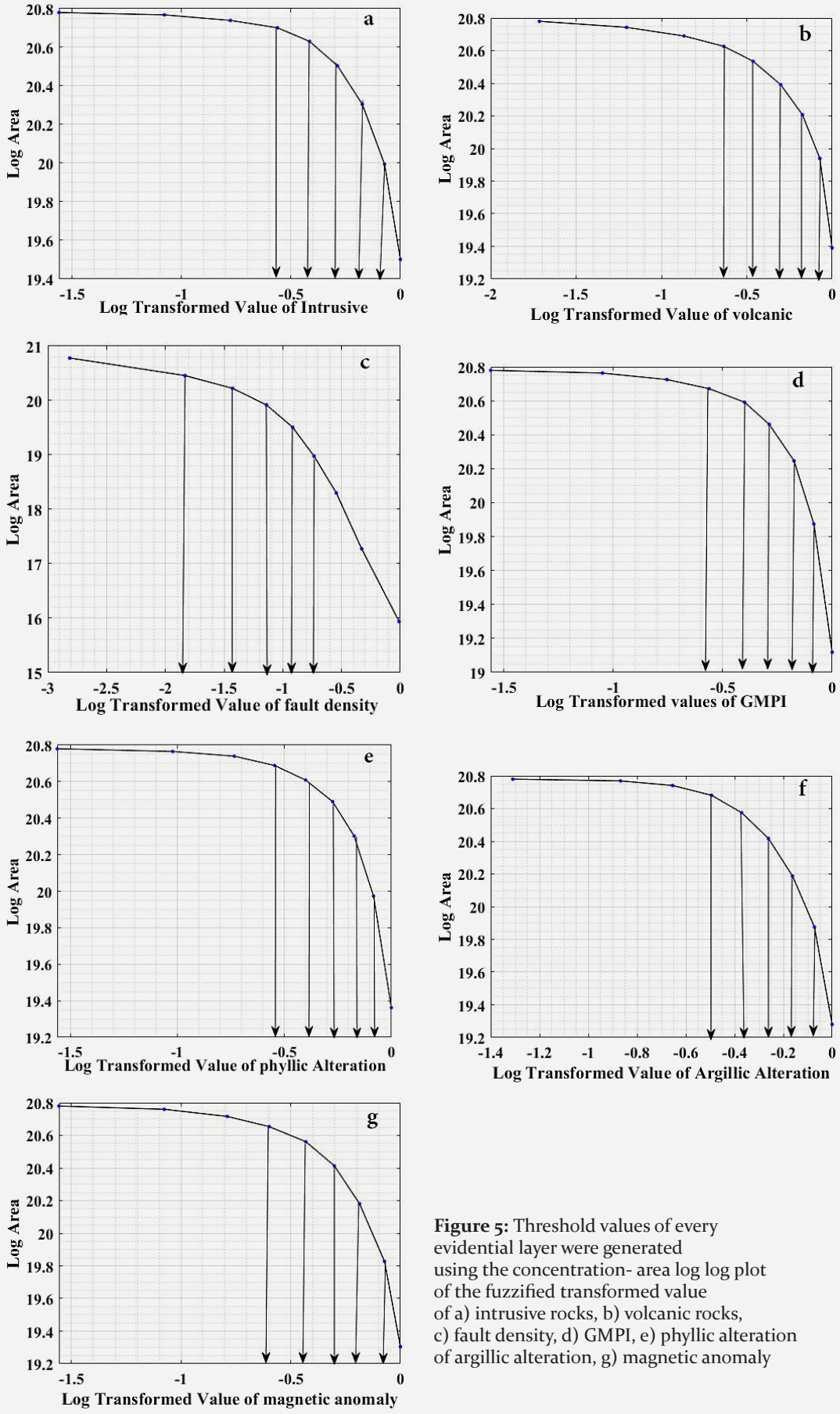

Figure 5: Threshold values of every evidential layer were generated using the concentration- area log log plot of the fuzzified transformed value of a) intrusive rocks, b) volcanic rocks, c) fault density, d) GMPI, e) phyllic alteration of argillic alteration, g) magnetic anomaly

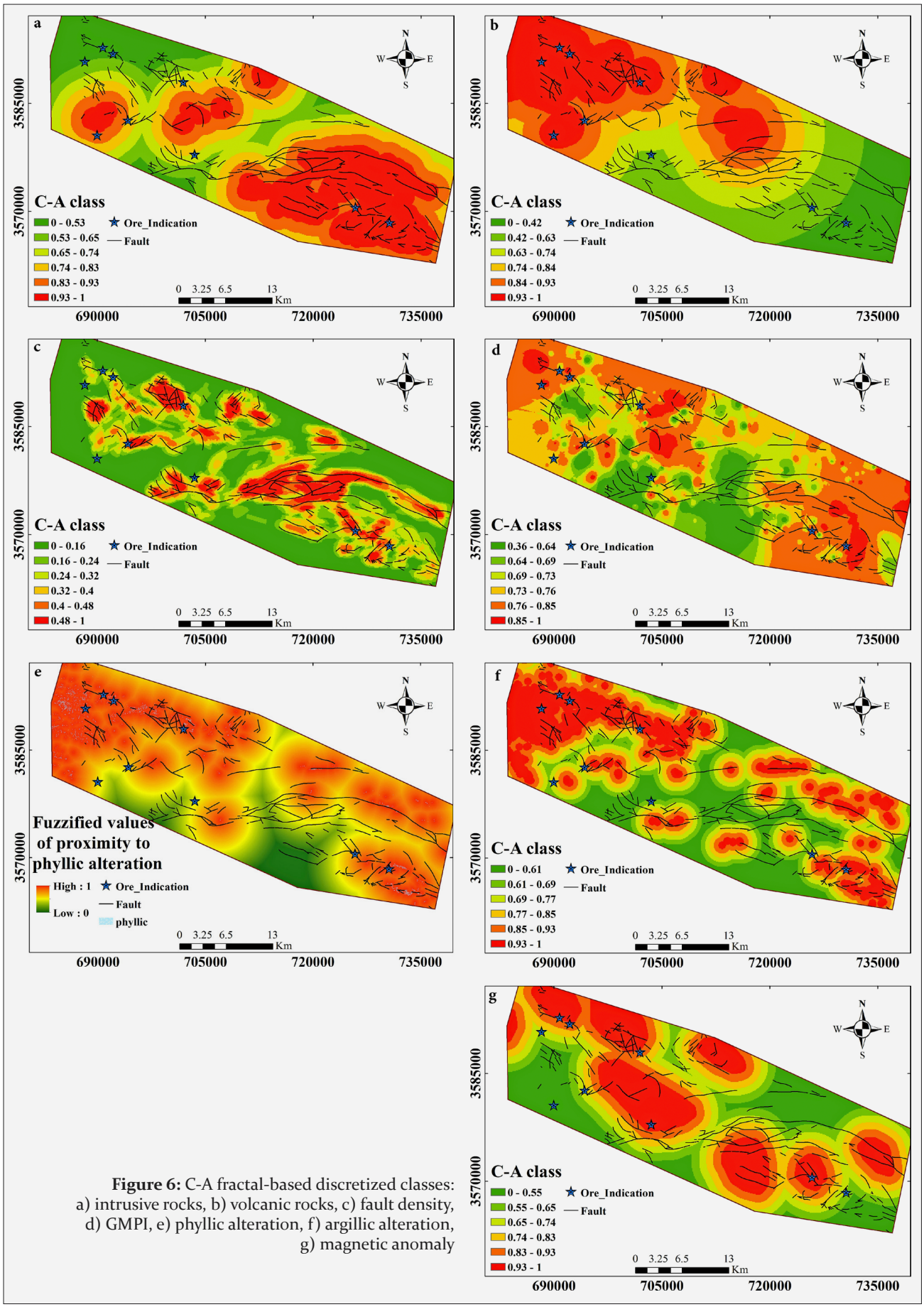

Figure 6: C-A fractal-based discretized classes: a) intrusive rocks, b) volcanic rocks, c) fault density, d) GMPI, e) phyllic alteration, f) argillic alteration, g) magnetic anomaly

Table 2: Pairwise comparison between seven main criteria of spatial databases and the weights produced using the AHP method

Criteria	GMPI	Argillic	Phylic	Geophysics	Intrusive	Volcanic	Fault	Weights
GMPI	1	1	2	3	3	4	5	0.264
Argillic	1	1	2	3	3	4	5	0.264
Phylic	0.5	0.5	1	2	2	3	4	0.162
Geophysics	0.33	0.33	0.5	1	2	3	4	0.124
Intrusive	0.33	0.33	0.5	0.5	1	2	3	0.09
Volcanic	0.25	0.25	0.33	0.33	0.5	1	2	0.066
Fault	0.2	0.2	0.25	0.25	0.33	0.5	1	0.03

Table 3: Pairwise comparison between sub-criteria (C-A fractal classes) of seven spatial databases and the weights resulted from the AHP method

Criteria	Classes	Weights	Criteria	Classes	Weights
GMPI	1	0.11	Geophysics	1	0.047
	2	0.07		2	0.031
	3	0.042		3	0.02
	4	0.026		4	0.013
	5	0.016		5	0.008
Argillic	1	0.1		6	0.005
	2	0.066	Intrusive	1	0.034
	3	0.042		2	0.022
	4	0.027		3	0.014
	5	0.017		4	0.009
	6	0.011		5	0.006
Phyllic	1	0.062		6	0.004
	2	0.04	Volcanic	1	0.022
	3	0.026		2	0.014
	4	0.017		3	0.009
	5	0.011		4	0.006
	6	0.007		5	0.004
Faults	1	0.015		6	0.002
	2	0.01			
	3	0.006			
	4	0.004			
	5	0.003			
	6	0.002			

and multivariate geochemical anomalies (Warg=0.264 and WGMPI=0.264). Proximity to the phyllic alteration was the next effective factor (Wp=0.162). The weight of proximity to geophysical anomalies was equal to 0.124 (Wgph=0.124). The weight of proximity to intrusive body was the next effective factor (Wint=0.09). The weight of proximity to volcanic rocks and faults density were the least important factors (Wvlc=0.066 and Wflt=0.03, respectively). All evidential layers were divided by the subcriteria using the fractal method and were weighted through the AHP method **(Table 3).** Then, the weights of criteria and subcriteria were used to distinguish favourable targets to porphyry copper modelling in the Mokhtaran area. Afterwards, the MATLAB package was used for weighting the decision matrix, coding AHP TOPSIS, AHP VIKOR and AHP MOORA. Then, the output matrix and codes were implemented to rank multi-dimensional alternatives. In the final stage, porphyry copper prospectivity models were generated. The three resulted models from AHP TOPSIS, AHP VIKOR and AHP MOORA are visualized.The threshold method was applied to draw high-potential areas. In order to obtain high potential areas, their threshold must first be obtained, in which the background and standard deviation value should be specified with the X+S equation **(Figure 8).**

9. Success rate curve

The performance of resulting favourability maps can be verified using the improved success rate curve. In a success rate curve, axis that is positioned horizontally shows the correctly categorized (PA) part of the study area and the axis that is positioned vertically describes the section of events related to the formation of minerals occurrences (PO) **(Ghezelbash and Maghsoudi, 2018).**

The current study applied the success rate curve for surveying and evaluating three prospectivity models, including AHP TOPSIS, AHP VIKOR, and AHP MOORA. The thresholds resulting from the fractal method were used to draw the success rate curve. All success rate curves were the upper gauge line **(Figure 9).** So, these prospectivity models are suitable to delineate favourable areas for Cu porphyry mineralization. The success rate curve showed that AHP TOPSIS has better applied in Cu porphyry modelling in the Mokhtaran area. This is because its success rate curve is above the other two methods. The AHP VIKOR method has had a better performance compared to the AHP MOORA method due to the fact that the success rate graph of the first mentioned is positioned higher than that of the second mentioned.

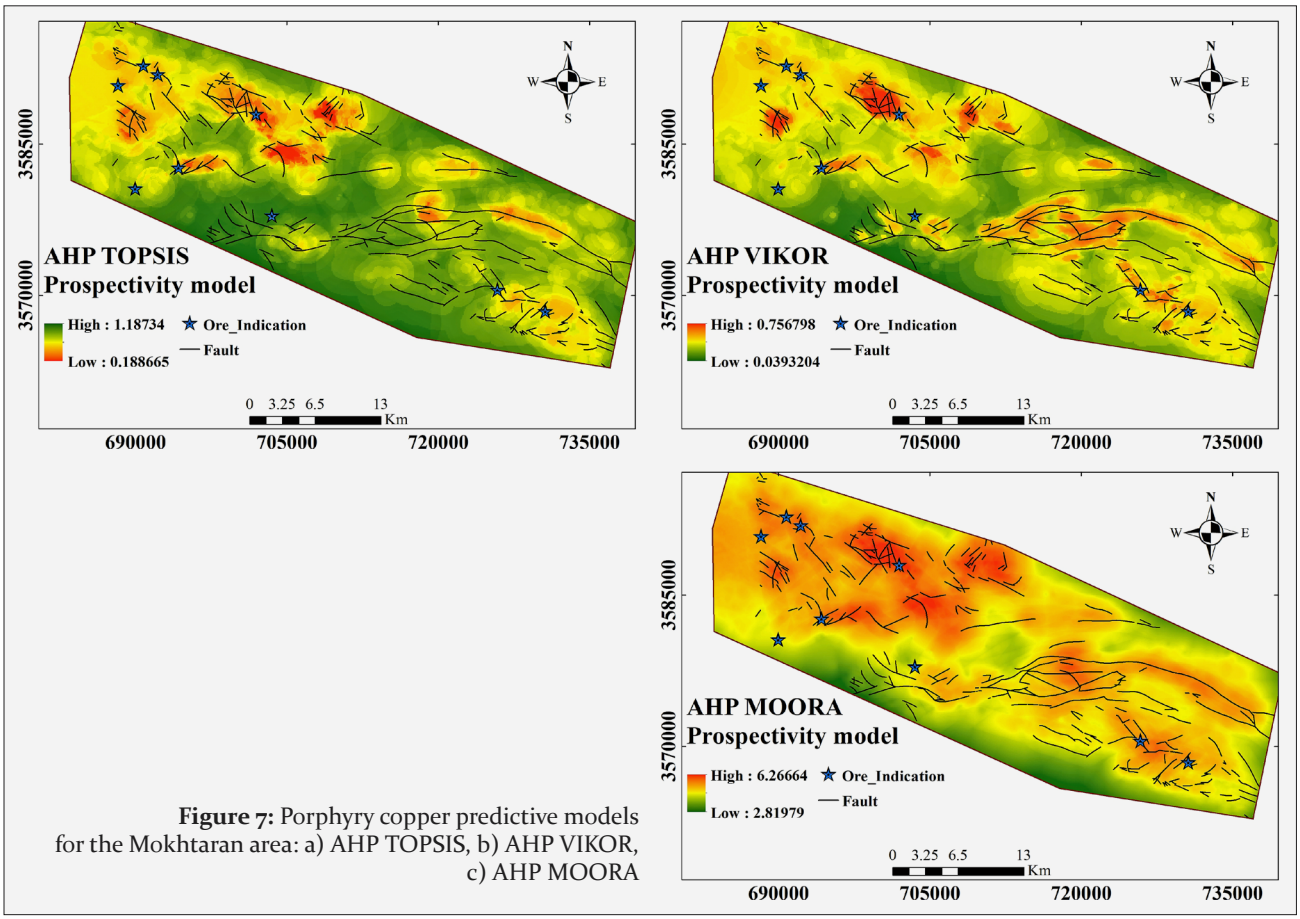

Figure 7: Porphyry copper predictive models for the Mokhtaran area: a) AHP TOPSIS, b) AHP VIKOR, c) AHP MOORA

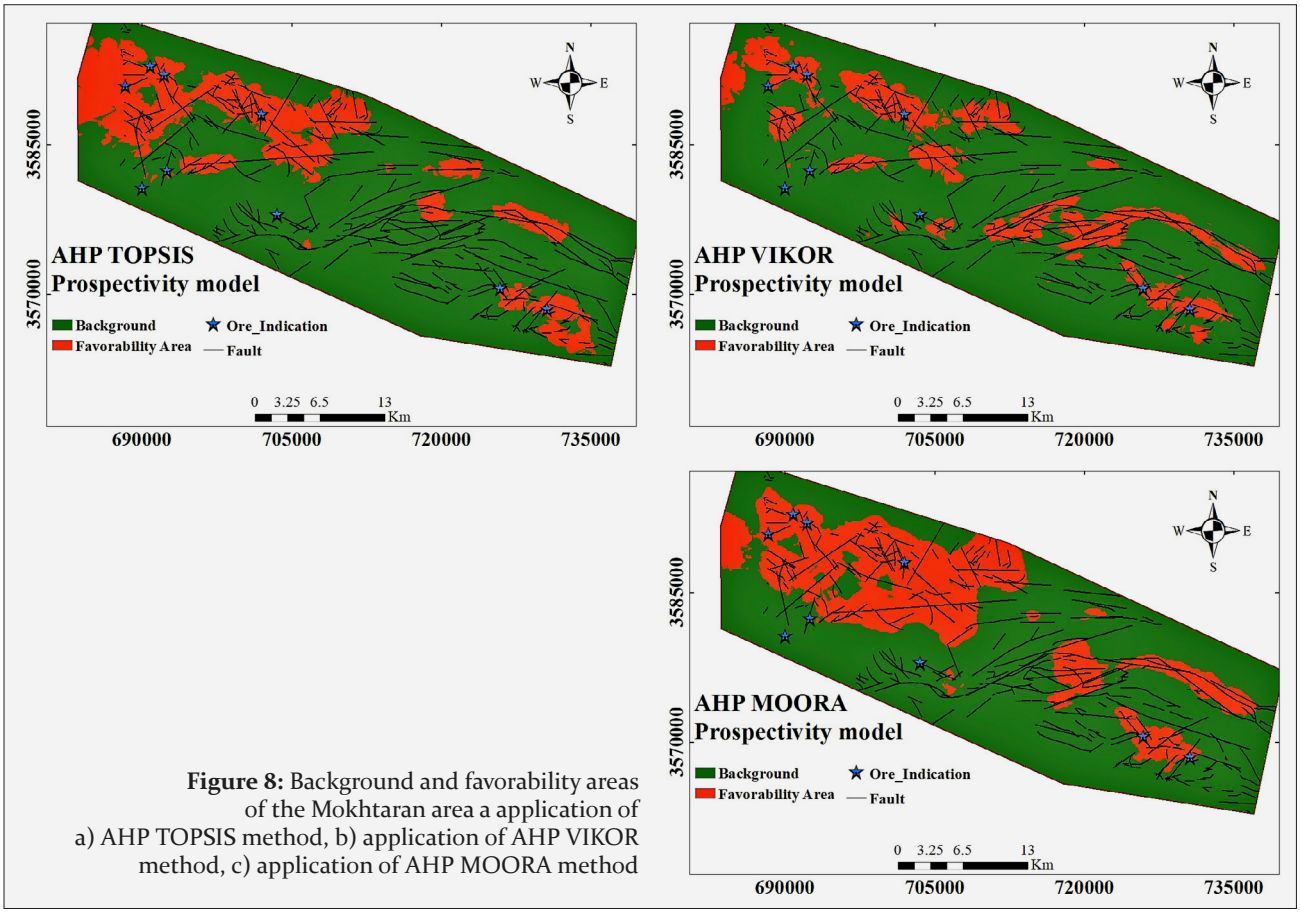

Figure 8: Background and favorability areas of the Mokhtaran area a application of a) AHP TOPSIS method, b) application of AHP VIKOR method, c) application of AHP MOORA method

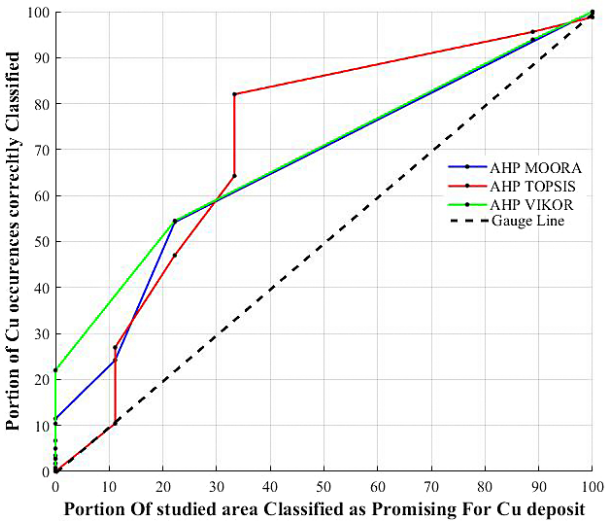

Figure 9: The success rate curve of three models

10. Discussion

The Mokhtaran region is in the Lut block in Eastern Iran. The Lut block is situated above the Afghan crust, and this region is associated with subduction. This zone has high potential for Cu-Au porphyry mineralization (**Karimpour et al., 2014**). This paper considers the mineral prospectivity modelling process an MCDM problem for porphyry copper modelling in the Mokhtaran area. To accomplish this objective, evidential geosptial datasets that encompass multiple disciplines of various sources consisting of geochemistry, geophysics, geology, and satellite images were used **(Table 1).** Then, we used three knowledge driven methods namely AHP TOPSIS, AHP VIKOR and AHP MOORA.

The geological data, including intrusive and volcanic rocks and faults, were digitized from the Mokhtaran 1:100K geology map and were converted into shapefiles. The alteration zones, consisting of argillic and phyllic alterations (**Figure 10)**, were processed from satellite imagery. The geochemical mineralization probability index (GMPI) was created from stream sediment geochemical data points in a raster format. Magnetic anomalies were extracted from the RTP magnetic map in shapefile formats. Secondly, the proximity map of every evidential layer was generated. The density map was generated only for lineaments, and the geochemical signature map was generated for the GMPI evidential layer. The evidential layers were transformed into the same scale using a fuzzy membership function, and continuous values of evidential layers were generated by equalizing minimum and maximum values **(Figure 3).** So, every evidential layer has the same value between zero and one. So, every evidential layer was transformed into a continuous geospatial dataset. Thirdly, the fractal method was implemented for separating the threshold values of fuzzified transformed evidential layers **(Figure 5).** All evidential layers were discretized to six subclasses. Fourthly, the calculated weights were assigned in the related evidential layers, and the weighted matrix was prepared to be imported to the MATLAB software. During this process, it was confirmed that the evidential layers could be integrated for mineral prospectivity modelling. In the next step, Cu porphyry prospectivity models were generated using the AHP TOPSIS, AHP VIKOR, and AHP MOORA MCDM methods. All MCDM prospectivity models produced similar prospectivity targets with high favourability. The high favourability areas in these three models coincide with fault zones, especially in fault intersection zones. These zones create fracture zones that are useful for the transportation of magmatic fluids to top levels that host the mineralized zones. This affirms the critical significance of faults in porphyry mineralization. However, the lowest weight was attributed to the fault density map. Then, the success rate curve was applied to evaluate the outcome of the three MCDM techniques. Based on the outcomes of the success rate curve, the AHP TOSIS performed better in Cu porphyry modelling in the Mokhtaran area.

11. Conclusions

Spatial data combination methods are essential ways in mineral deposit modelling. In this paper, seven evidential layers including geological units and structures, geochemistry, geophysics, and remote sensing, as well as the MCDM methods consisting of AHP TOPSIS, AHP VIKOR, and AHP MOORA were applied for Cu porphyry modelling in the Mokhtaran area, east of Iran. The success rate curve method was used to assess Cu porphyry models. The three Cu porphyry models resulted from the MCDM methods are similar to each other. The study area contains promising locations in both its

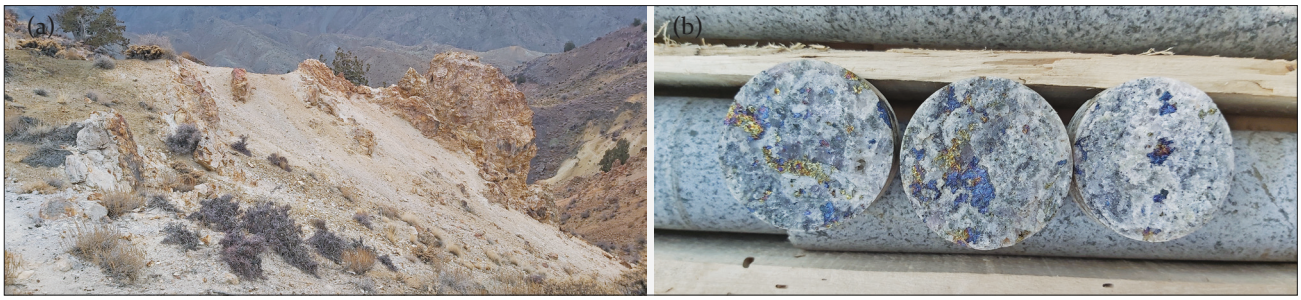

Figure 10: a) Argillic alteration, b) Porphyry mineralization

eastern and western regions. The promising areas are located along the fault zones, confirming the role of faults and fractured zones in Cu porphyry systems. Several Cu indications were properly identified using the three MCDM methods, but AHP TOPSIS showed better results. According to the success rate curve, the positions of the three models' curves are higher than the gauge line. Therefore, all of the models are appropriate. However, the AHP TOPSIS method exhibits a success rate curve that surpasses the curves of the other two methods. Therefore, it can be concluded that AHP TOPSIS outperformed the other methods in Cu porphyry modelling in the Mokhtaran area. Also, the following results were obtained in this study :

All three methods, AHP TOPSIS, AHP VIKOR, and AHP MOORA, have the ability to distinguish areas with high porphyry copper mineralization potential. These three methods are able to convert the qualitative values of experts› knowledge into quantitative values for porphyry copper potential. Also, the models produced by these three methods confirm the existence of areas with high mineralization potential, which can be effective for more surface exploration in the future.

12. References

Abedi, M., Mohammadi, R., Norouzi, G.H., Mohammadi, M. (2016): A comprehensive VIKOR method for integration of various exploratory data in mineral potential mapping. Arabian Journal of Geosciences, 9(6):482.

Afzal, P., Harati, H., Fadakar, Y., Yasrebi A. (2013): Application of spectrum–area fractal model to identify of geochemical anomalies based on soil data in Kahang porphyry-type Cu deposit, Iran. Geochemistry, 73(4):533-543.

Albayrak, E., Erensal, Y. (2004): Using analytic hierarchy process (AHP) to improve human performance: an application of multiple criteria decision-making problem. Journal of Intelligent Manufacturing, 15:491–503

Almasi, A., Nabatian, G., Mahdavi, A., & Li, Q. (2023): High degree partial melting of the metasomatized mantle: a possible source for the Eocene-Oligocene porphyry Cu-Au-Mo deposits in Lut block, Eastern Iran. Ore Geology Reviews, 157, 105386.

Arian, H., Ashkan, H. (2015): Comprehensive MULTI-MOORA method with target-based attributes and integrated significant coefficients for materials selection in biomedical applications, Materials & Design, 87 -949–959.

Cheng, Q., Agterberg, F. P., Ballantyne, S. B. (1994): The separation of geochemical anomalies from background by fractal methods. Journal of Geochemical Exploration, 51 (2): 109-130.

Coope, A. (1973); Geochemical prospecting for porphyry copper-type mineralization — A review, Journal of Geochemical Exploration, 2, Issue 2, 81-102.

Du, X., Zhou, K., Cui, Y., Wang, J., Zhou, S. (2021): Mapping Mineral Prospectivity Using a Hybrid Genetic Algorithm–Support Vector Machine (GA–SVM) Model. ISPRS International Journal of Geo-Information, 10, 766.

Epithermal gold deposits in the circum-pacific region. Australian Journal of Earth Sciences, 44, 373–388.

Esmaeilzadeh, A., Khademi, D., Mikaeil, R., Taghizadeh, S. (2021): 'The Use of VIKOR Method to Set up Place Locating of Processing Plant (Case Study: Processing Plant of South of West Azerbaijan)', Journal of Soft Computing in Civil Engineering, 5(1), 38-48.

Feizi, F., Karbalaei, A., Farhadi, S. (2021): FUCOM-MOORA and FUCOM-MOOSRA: new MCDM-based knowledge-driven procedures for mineral potential mapping in greenfields. SN Applied Sciences, 3, 358.

Ghezelbash, R., Maghsoudi, A. (2018): A hybrid AHP-VIKOR approach for prospectivity modeling of porphyry Cu deposits in the Varzaghan District, NW Iran. Arabian Journal of Geosciences, 11, 275.

Heidari, M., Ghaderi, M., Afzal, P. (2013): Delineating mineralized phases based on lithogeochemical data using multifractal model in Touzlar epithermal Au–Ag (Cu) deposit, NW Iran, Applied Geochemistry, 31, 119-132.

Hou, Z., Xiaofei Z., Yang., Z. (2011): Porphyry Cu (–Mo–Au) deposits related to melting of thickened mafic lower crust: Examples from the eastern Tethyan metallogenic domain, Ore Geology Reviews, 39, 1–2, 21-45.

Karimpour, M., Mazhari, N., Shafaroudi, A. (2014): Discrimination of Different Erosion Levels of Porphyry Cu Deposits using ASTER Image Processing in Eastern Iran: a Case Study in the Maherabad, Shadan, and Chah Shaljami Areas. Acta Geologica Sinica (English Edition), 88, 1195-1213.

Li, S., Chen, J., Liu, C. (2022): Overview on the Development of Intelligent Methods for Mineral Resource Prediction under the Background of Geological Big Data. Minerals, 12, 616.

Pan, C., Harris, D. (2000): Information Synthesis for Mineral Exploration, Oxford University Press, New York, NY, USA, p. 461.

Parsa, M., Maghsoudi, A., Yousefi, M., Sadeghi, M. (2016): Recognition of significant multi-element geochemical signatures of porphyry Cu deposits in Noghdouz area, NW Iran. Journal of Geochemical Exploration, 165, 111–124.

Procedia Computer Science, 55, 1123-1132.

Riahi, S., Bahroudi, B., Abedi, M., Lentz, D., Aslani, S. (2023): Application of data-driven multi-index overlay and BWM-MOORA MCDM methods in mineral prospectivity mapping of porphyry Cu mineralization, Journal of Applied Geophysics, 213, 105025.

Richards, P. (2011): Magmatic to hydrothermal metal fluxes in convergent and collided margins, Ore Geology Reviews, 40, 1, 1-26,

Robbi, R., Supiyandi, S., Andysah, S., Tri, S., Andy, S., Wiwit, T., Yudie, I., Siti, A., Mufida, K., Siti, S., Khairunnisa, K. (2018): TOPSIS Method Application for Decision Support System in Internal Control for Selecting Best Employees. Journal of Physics: Conference Series. 1028. 012052.

Rosaria, R., Camanho, R. (2015): Criteria in AHP: A Systematic Review of Literature.

Saaty TL. (1977): A scaling method for priorities in hierarchical structures.

Saljoughi, B., Hezarkhani, A., Farahbakhsh, E. (2018): A comparison between knowledge-driven fuzzy and data-driven

artificial neural network approaches for prospecting porphyry Cu mineralization; a case study of Shahr-e-Babak area, Kerman Province, SE Iran, Journal of Mining & Environment: 9(4): 917-940.

Shafaroudi, A., Karimpour, M., Stern, C. (2015): The Khopik porphyry copper prospect, Lut Block, Eastern Iran: Geology, alteration and mineralization, fluid inclusion, and oxygen isotope studies, Ore Geology Reviews, 65 (2), 522-544.

Siahaan, A., Dodi, S., Darmawan, N. (2018): Multi-Attribute Decision Making with VIKOR Method for Any Purpose Decision, Journal of Physics: Conference Series. 10.31227/osf.io/2m8x4.

Sillitoe, R., (1997). Characteristics and controls of the largest porphyry copper-gold and epithermal gold deposits in the circum-Pacific region. Australian Journal of Earth Sciences, 44(3), 373–388.

Sillitoe, R. (1973): The tops and bottoms of porphyry copper deposits. Economic Geology, 68 (6): 799–815.

Sillitoe, R. (2010): Porphyry Copper Systems. Economic Geology, 105 (1): 3–41.

Sinclair, W.D. (2007): Porphyry Deposits. In: Goodfellow, W.D., Ed., Mineral Deposits of Canada: A Synthesis of Major Deposit-Types, District Metallogeny, the Evolution of Geological Provinces, and Exploration Methods, Geological Association of Canada, Mineral Deposits Division, Special Publication, Canada, Newfoundland, 223-243.

Yousefi, M., Kamkar-Rouhani, A., Carranza, E. (2012): Geochemical mineralization probability index (GMPI): A new approach to generate enhanced stream sediment geochemical evidential map for increasing probability of success in mineral potential mapping, Journal of Geochemical Exploration, 115, 24-35.

SAŽETAK

Metode vođene znanjem za modeliranje potencijala Cu-Au porfira; studija slučaja područja Mokhtaran, istočni Iran

Trenutačna istraživanja za modeliranje potencijala porfirskoga bakra u području Mokhtaran u istočnome Iranu istražuju metode odlučivanja po više kriterija, a one uključuju AHP TOPSIS, AHP VIKOR i AHP MOORA. Dokazni slojevi u ovoj studiji uključuju intruzivne stijene, vulkanske stijene, rasjede, indeks vjerojatnosti geokemijske mineralizacije (GMPI), redukciju na magnetski pol karte ukupnoga magnetskog intenziteta, argilne i filne alteracije. Važnost tih dokaznih slojeva izračunana je AHP metodom. Zatim je *fuzzy* metoda primijenjena na istu ljestvicu dokaznih slojeva. Granične vrijednosti tih slojeva diskretizirane su fraktalnom metodom. Zatim je svakom sloju dokaza dodijeljena težina. Nakon vaganja svih slojeva dokaza implementirane su različite metode MCDM, uključujući AHP TOPSIS, AHP VIKOR i AHP MOORA, kako bi se kombinirali ti slojevi i ocrtali modeli perspektivnosti porfirskoga bakra. Predviđeni modeli pokazuju ista područja koja obećavaju. Odgovarajuća podudarnost može se vidjeti između područja visokoga potencijala i indikacija rudnika. Zatim je implementirana stopa krivulje uspješnosti za usporedbu triju predviđenih modela. Na temelju ove metode AHP TOPSIS ima bolje performanse. Budući da krivulja uspješnosti pripada AHP TOPSIS-u, postavljena je iznad drugih dviju metoda. Dalje, AHP VIKOR ima bolje performanse od AHP MOORA. Tri metode MCDM proizvele su istu Cu porfirsku mineralizaciju koja se nalazi duž rasjednih zona.

Ključne riječi:
AHP, MOORA, VIKOR, Mokhtaran, porfir

Author's contributions

All authors contributed to the study conception and design. Data collection and modeling were performed by **Moslem Jahantigh (1)** (PHD candidate, mineral exploration department, Amirkabir university of technology) candidate and **Hamidreza Ramazi (2)** (Professor, mineral exploration department, Amirkabir university of technology). The first draft of the manuscript was written by Moslem Jahantigh. Hamid Reza Ramazi read and approved the final manuscript.